On the Out-of-Plane Vibration of Rotating Circular Nanoplates

WANG Xinyue[1] , LUO Qiuyang[1] , LI Cheng[1] , XIE Zhongyou[2]*

1. School of Rail Transportation, Soochow University, Suzhou 215131, P.R. China;

2. School of Architectural Engineering, Tongling University, Tongling 244061, P.R. China

Abstract: A rotating axisymmetric circular nanoplate is modeled by the Mindlin plate theory. The Mindlin plate theory incorporates the nonlocal scale and strain gradient effects. The shear deformation of the circular nanoplate is considered and the nonlocal strain gradient theory is utilized to derive the governing differential equation of motion that describes the out-of-plane free vibration behaviors of the nanoplate. The differential quadrature method is used to solve the governing equation numerically, and the natural frequencies of the out-of-plane vibration of rotating nanoplates are obtained accordingly. Two kinds of boundary conditions are commonly used in practical engineering, namely the fixed and simply supported constraints, and are considered in numerical examples. The variations of natural frequencies with respect to the thickness to radius ratio, the angular velocity, the nonlocal characteristic scale and the material characteristic scale are analyzed in detail. In particular, the critical angular velocity that measures whether the rotating circular nanoplate is stable or not is obtained numerically. The presented study has reference significance for the dynamic design and control of rotating circular nanostructures in current nano-technologies and nano-devices.

Key words: circular nanoplate; nonlocal strain gradient; differential quadrature method; material characteristic scale; angular velocity

CLC number: O324   **Document code:** A   **Article ID:** 1005-1120(2022)01-0023-13

0 Introduction

With the rapid development of nanotechnology, the materials and structures at a nanoscale have attracted increasing attentions during the past two decades[1-3]. As a new research field, nanotechnology involves the property, optimization and application of materials with scales between 1 nm and 100 nm, including nanoelectronics, nanophotonics, nanobiology, nanomedicine and other branch subjects, among which the mechanical property of nanomaterials and nanostructures, i.e., the nanomechanics plays an important role. The mechanical characterizations with related nanoscale properties and parameters are indispensable in the preparation, testing, modification and optimization of nanomaterials[4]. Stationary nanomaterials and nanostructures are currently characterized and tested easily but requires a static condition. Performance characterization under motion is one of the technical difficulties, which hinders the development of new nanomaterials and functional structures based on kinetic design[5]. Therefore, it has important scientific significance in studying the mechanical properties of nanomaterials and nanostructures, especially the dynamic properties of those with motion. Regarding the research methodologies, theoretical approaches and corresponding models and analyses are more popular in view of the complexity of manipulation and testing of nanoscale dynamic experiments[6]. The theoretical approaches are mainly divided into two categories. One is the discrete atomic model[7]. By regarding nanomaterials as an integration of a certain number of atoms, the discrete model of nano-

materials is established by considering the forces between atoms. The other is the non-classical continuum model[8] that regards nanomaterials as a generalized continuum and accounts for the internal characteristic scale parameters of materials. However, when the number of atoms compose nanomaterials and nanostructures is relatively large, the discrete model is cumbersome in both modeling and calculation. For instance, the calculation costs extra hardware and long time. With the requirements of analyzing complex nanosystems, the non-classical continuum model dominates the theoretical prediction of dynamic phenomena in nanomaterials and nanostructures.

For non-classical continuum models, since the beginning of the last century, the couple stress theory and its modified versions, the micropole and microstate theory, the strain gradient theory, the nonlocal theory, and the nonlocal strain gradient theory have been proposed successively[9]. These theoretical methods have been applied to the analysis of mechanical properties of nanostructures during past years. For instance, Akgöz et al.[10] proposed a size-dependent higher-order shear deformation beam model based on the Navier method and the modified strain gradient theory in which both the microstructural and shear deformation effects were taken into consideration. Akgöz et al.[11] studied the thermomechanical buckling behaviors of embedded functionally graded microbeams based on the sinusoidal shear deformation beam theory and modified couple stress theory. Numanoğlu et al.[12] investigated the longitudinal dynamic properties of nanorods with various boundary conditions based on the nonlocal theory. Ebrahimi et al.[13] developed a nonlocal couple stress theory to reveal the vibration behaviors and stabilities of functionally graded nanobeams using the Chebyshev-Ritz method. Nevertheless, there are still some unsolved problems in the theoretical application. For example, the micro-softening and hardening predictions were contradicted[14], and the undefined or inconsistent internal characteristic scale parameters[15] were used in previous studies. In regard of these, Lim et al.[16] established a nonlocal strain gradient theory in 2015, which introduced and coupled both the nonlocal parameter and material characteristic scale parameter to measure the nonlocal effect and strain gradient effect of nanomaterials and structures, respectively. Accordingly, the total nonlocal strain gradient stress is defined, and the constitutive relations reflect the nonlocal effect of classical strains and strain gradients, as well as the gradient effect of nonlocal stresses and total stresses, which promotes the application adaptability of the nonlocal strain gradient theory at a nanoscale. Meanwhile, it has been proved that the micro-softening and hardening phenomena are observed and in fact they are described by two special cases of the theory, namely, corresponding to two simplified forms of the theory[17]. Moreover, it also has the guiding significance for the determination of the internal characteristic scale parameters in the non-classical continuum theory[18]. Consequently, the nonlocal strain gradient theory is suitable for the study of nanomechanics. This is why it has became a popular research method in nanomechanics since the theory was put forward[19-24]. In this paper, the nonlocal strain gradient theory is used to examine the vibration behavior of circular nanoplates.

The vibration and stability of axially moving nanostructures have been fully studied during the past several years[25-30]. However, rotating nanostructures are relatively less studied. The rotating circular nanoplate is one of the important components in the nanoelectromechanical system[31] that is usually used to realize power and motion transmissions. Hence it is a common structure for the system operation. To solve the vibration equations to show dynamic behaviors and other related characteristics of the circular nanoplates, the differential quadrature method and the nonlocal finite element method are usually used[32-34]. Generally, the structural characteristics, forces and constraints of circular nanoplates are axisymmetric. Therefore, the present work concerns the free vibration characteristics of axisymmetric circular nanoplates with rotational motion. The results may provide a theoretical basis for the dynamic design and optimization of key components in the nanoelectromechanical system.

1 Theory and Method

1. 1 Nonlocal strain gradient theory

The nonlocal strain gradient theory combines the higher-order stress gradients with the nonlocal effect of strain gradients. The constitutive relations can be expressed as[16]

$$
\begin{cases}
\boldsymbol{\sigma} = \int_V \alpha_0 \left(\boldsymbol{x}', \boldsymbol{x}, e_0 a \right) \boldsymbol{C} : \boldsymbol{\varepsilon}' \mathrm{d} V' \\
\boldsymbol{\sigma}^{(1)} = l^2 \int_V \alpha_1 \left(\boldsymbol{x}', \boldsymbol{x}, e_1 a \right) \boldsymbol{C} : \nabla \boldsymbol{\varepsilon}' \mathrm{d} V' \\
\boldsymbol{t} = \boldsymbol{\sigma} - \nabla \boldsymbol{\sigma}^{(1)}
\end{cases}
\tag{1}
$$

where $\boldsymbol{\sigma}$ and $\boldsymbol{\sigma}^{(1)}$ represent the nonlocal stress tensor and the higher-order nonlocal stress tensor in volume V, respectively; α_0 and α_1 the nonlocal kernel functions related to the strain and the first-order strain gradient; and e_0 and e_1 the traditional nonlocal and higher-order nonlocal material constants. $\boldsymbol{t}$ represents the nonlocal strain gradient total stress tensor; $\boldsymbol{C}$ the elastic tensor; $\boldsymbol{\varepsilon}'$ the strain tensor at point $\boldsymbol{x}'$; a the nonlocal characteristic scale; l the material characteristic scale related to higher-order strain gradients; and ∇ the gradient operator. As a result, the nonlocal stress and higher-order nonlocal stress at point $\boldsymbol{x}$ depends on not only the strain and strain gradient at point $\boldsymbol{x}$, but also the strain and strain gradient at point $\boldsymbol{x}'$ in the nonlocal strain gradient theory. That is, the idea of long-range interactions between molecules/atoms is introduced into both the nonlocal and strain gradient constitutive relations.

The above integral constitutive equations are difficult to solve. Fortunately, they can be transformed into differential constitutive equations. Based on certain assumptions, the core constitutive relation of the nonlocal strain gradient theory can be simplified by reorganizing the integral constitutive equations and introducing the Laplace operator as[16]

$$
\left[1 - (ea)^2 \nabla^2 \right] t_{xx} = E (1 - l^2 \nabla^2) \varepsilon_{xx}
\tag{2}
$$

where ∇^2 is the Laplace operator, and two material constants are assumed to be identical, i.e. $e_0 = e_1 = e$.

1. 2 Differential quadrature method

There are different methods to solve differential equations, among which the differential quadrature method has been widely used due to its fast cal-culation and high accuracy. In this numerical method, the function values of all nodes in the whole domain are weighted and summed to represent the function value and its derivatives at the selected node. Resultingly, the differential equations can be discretized into a set of algebraic equations with the node values as the unknown variables. For a one-dimensional function $f(x)$, let it be continuously differentiable in the interval $[a, b]$, and one obtains

$$
L\left\{ f(x) \right\} = \sum_{m=1}^{N} W_m(x) f(x_m)
\tag{3}
$$

where L is a linear differential operator; $W_m(x)$ the interpolation basis function; and x_m the mth node in the interval $[a, b]$.

Let $\quad L = \dfrac{\mathrm{d}}{\mathrm{d}x}, \quad C_{jm}^{(1)} = W_m(x_j), \quad f_m = f(x_m),$ then

$$
Lf(x_j) = \frac{\mathrm{d} f(x_j)}{\mathrm{d}x} = f_j^{(1)} = \sum_{m=1}^{N} C_{jm}^{(1)} f_m
\tag{4}
$$

where $j = 1, 2, \cdots, N$, and $C_{jm}^{(1)}$ is the first-order weighting coefficient of function $f(x)$. Accordingly, $\left[C_{jm}^{(1)} \right]$ is the weighting coefficient matrix of its first derivative.

Denote $f_j^{(k)} = f^{(k)}(x_j)$, then the higher-order derivative at the function node can be represented by the interpolation of function values as

$$
\frac{\mathrm{d}^2 f(x_j)}{\mathrm{d}x^2} = f_j^{(2)} = \sum_{m=1}^{N} C_{jm}^{(2)} f_j
\tag{5}
$$

$$
\frac{\mathrm{d}^3 f(x_j)}{\mathrm{d}x^3} = f_j^{(3)} = \sum_{m=1}^{N} C_{jm}^{(3)} f_j
\tag{6}
$$

$$
\frac{\mathrm{d}^4 f(x_j)}{\mathrm{d}x^4} = f_j^{(4)} = \sum_{m=1}^{N} C_{jm}^{(4)} f_j
\tag{7}
$$

where $C_{jm}^{(2)}$, $C_{jm}^{(3)}$ and $C_{jm}^{(4)}$ are the weighting coefficients of the second, the third, and the fourth derivatives of function $f(x)$. Accordingly, the higher-order derivative can be regarded as the derivation of the first-order derivative.

To determine the weight coefficients, let $f(x) = x^{k-1}$, the following formula can be obtained from Eq.(4) as

$$
(k-1) x_j^{k-2} = \sum_{m=1}^{N} C_{jm}^{(1)} x_m^{k-1}
\tag{8}
$$

Eq.(8) can be written in a matrix form as $\boldsymbol{G} = \boldsymbol{C} \boldsymbol{V}$, where

$$G = \begin{bmatrix} 0 & 1 & 2x_1 & \cdots & (N-1)x_1^{N-2} \\ 0 & 1 & 2x_2 & \cdots & (N-1)x_2^{N-2} \\ & & & & \\ 0 & 1 & 2x_N & \cdots & (N-1)x_N^{N-2} \end{bmatrix}_{N \times N} \quad (9)$$

$$V = \begin{bmatrix} 1 & x_1 & \cdots & x_1^{N-2} \\ 1 & x_2 & \cdots & x_2^{N-2} \\ & & & \\ 1 & x_N & \cdots & x_N^{N-2} \end{bmatrix}_{N \times N} \quad (10)$$

Lagrange interpolation can be used as the expression of a function node

$$f(x) = \sum_{m=1}^{N} l_m(x) f(x_m) \quad (11)$$

where $l_m(x)$ is the Lagrange interpolation polynomial as

$$l_m(x) = \prod_{\substack{k=1 \\ k \neq m}}^{N} \frac{x - x_k}{x_m - x_k} \quad (12)$$

The first derivative of Eq.(11) is

$$f'(x) = \sum_{m=1}^{N} l_m'(x) f \quad (13)$$

Consequently

$$f_j' = f'(x_j) = \sum_{m=1}^{N} l_m'(x_j) f \quad (14)$$

Comparing Eq.(4) and Eq.(14), we can get

$$C_{jm}^{(1)} = l_m'(x_j) \quad (15)$$

Therefore, the explicit expressions of the first-order and higher-order weight coefficients can be determined. Furthermore, a reasonable node distribution should be selected while using the differential quadrature method. The previous studies[32] show that the roots of Chebyshev polynomial can make the calculation faster with more accurate. Therefore, it is adopted in the present study as

$$x_m = \frac{1}{2}\left[1 - \cos\left(\frac{m-1}{N-1}\pi\right)\right] \quad (16)$$

2 Problem Model and Governing Equation

Considering an axisymmetric circular nanoplate rotating at an angular velocity Ω, with a radius R and thickness h, we establish a polar coordinate system, as shown in Fig.1, where z-coordinate is along the axis (i.e. thickness direction) of the circular nanoplate.

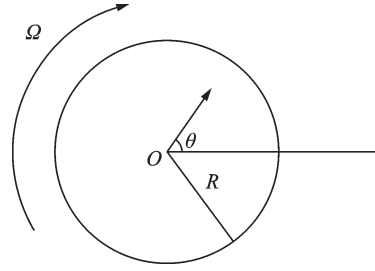Based on the Mindlin plate theory, the radial

Fig.1   Diagrammatic sketch of an axisymmetric rotating circular nanoplate

displacement u_r and lateral displacement u_z of the circular nanoplate can be expressed as

$$\begin{cases} u_r(r,z,t) = z\varphi(r,t) \\ u_z(r,z,t) = w(r,t) \end{cases} \quad (17)$$

where $w(r,t)$ represents the lateral displacement of any point on the midplane; $\varphi(r,t)$ the rotational angle of the midplane normal; and t the time.

From Eq.(17), the geometric equation can be obtained as

$$\varepsilon_r = z\frac{\partial \varphi}{\partial r}, \quad \varepsilon_\theta = z\frac{\varphi}{r}, \quad \gamma_{rz} = \varphi + \frac{\partial w}{\partial r} \quad (18)$$

Considering Eq.(18) together with the physical equation, one can obtain the classical stress components as

$$\sigma_r = \frac{E}{1-\nu^2}(\varepsilon_r + \nu\varepsilon_\theta) = \frac{E}{1-\nu^2}\left[z\frac{\partial \varphi}{\partial r} + \nu\frac{z}{r}\varphi\right] \quad (19)$$

$$\sigma_\theta = \frac{E}{1-\nu^2}(\nu\varepsilon_r + \varepsilon_\theta) = \frac{E}{1-\nu^2}\left[z\nu\frac{\partial \varphi}{\partial r} + \frac{z}{r}\varphi\right] \quad (20)$$

$$\tau_{rz} = \frac{E}{2(1+\nu)}\gamma_{rz} = \frac{E}{2(1+\nu)}\left(\varphi + \frac{\partial w}{\partial r}\right) \quad (21)$$

where ε_r, ε_θ and γ_{rz} are the radial strain, the hoop strain and the shear strain, respectively; σ_r, σ_θ and τ_{rz} the radial stress, the hoop stress and the transverse shear stress, respectively; and E and ν the elastic modulus and the Poisson's ratio, respectively. Subsequently, the internal forces including the axial force, the bending moment and the transverse shear force can be obtained by integrating Eqs.(19—21). Therefore, the constitutive equations based on the nonlocal strain gradient theory can be derived

$$\left[1 - (ea)^2 \nabla^2\right]N_r = \int_{-\frac{h}{2}}^{\frac{h}{2}} \sigma_r \mathrm{d}z = B_1\left(\frac{\partial \varphi}{\partial r} + \nu\frac{\varphi}{r}\right) \quad (22)$$

$$\left[1 - (ea)^2 \nabla^2\right]N_\theta = \int_{-\frac{h}{2}}^{\frac{h}{2}} \sigma_\theta \mathrm{d}z = B_1\left(\nu\frac{\partial \varphi}{\partial r} + \frac{\varphi}{r}\right) \quad (23)$$

$$\left[1-(ea)^2\nabla^2\right]M_r=\int_{-\frac{h}{2}}^{\frac{h}{2}}\sigma_r z\mathrm{d}z=$$

$$(1-l^2\nabla^2)\left[D_1\left(\frac{\partial\varphi}{\partial r}+\nu\frac{\varphi}{r}\right)\right] \qquad (24)$$

$$\left[1-(ea)^2\nabla^2\right]M_\theta=\int_{-\frac{h}{2}}^{\frac{h}{2}}\sigma_\theta z\mathrm{d}z=$$

$$(1-l^2\nabla^2)\left[D_1\left(\nu\frac{\partial\varphi}{\partial r}+\frac{\varphi}{r}\right)\right] \qquad (25)$$

$$\left[1-(ea)^2\nabla^2\right]Q_r=\int_{-\frac{h}{2}}^{\frac{h}{2}}\tau_{rz}\mathrm{d}z=$$

$$(1-l^2\nabla^2)\frac{S_1}{\kappa}\left(\varphi+\frac{\partial w}{\partial r}\right) \qquad (26)$$

$$B_1=\int_{-\frac{h}{2}}^{\frac{h}{2}}\frac{Ez}{1-\nu^2}\mathrm{d}z=0 \qquad (27)$$

$$D_1=\int_{-\frac{h}{2}}^{\frac{h}{2}}\frac{E}{1-\nu^2}z^2\mathrm{d}z=\frac{Eh^3}{12(1-\nu^2)} \qquad (28)$$

$$S_1=\int_{-\frac{h}{2}}^{\frac{h}{2}}\frac{E}{2(1+\nu)}\mathrm{d}z=\frac{Eh}{2(1+\nu)} \qquad (29)$$

where N_r and N_θ are the components of the axial force; and M_r and M_θ the components of the bending moment. Q_r is the transverse shear force, and $\kappa=12/\pi^2$ the shear correction factor[35].

The first-order variation of the strain energy U of the rotating axisymmetric circular nanoplate can be calculated as

$$\delta U=\delta\int_v\frac{1}{2}\left(\sigma_r\varepsilon_r+\sigma_\theta\varepsilon_\theta+\tau_{rz}\gamma_{rz}\right)\mathrm{d}V=$$

$$\int_v\left[\left(\sigma_r z\delta\frac{\partial\varphi}{\partial r}\right)+\left(\sigma_\theta z\frac{\delta\varphi}{r}\right)+\right.$$

$$\left.\left(\tau_{rz}\delta\varphi+\tau_{rz}\delta\frac{\partial w}{\partial r}\right)\right]\mathrm{d}V=$$

$$\int rM_r\delta\varphi\Big|_0^R\mathrm{d}\theta-\iint\frac{\partial(rM_r)}{\partial r}\delta\varphi\mathrm{d}r\mathrm{d}\theta+$$

$$\iint M_\theta\delta\varphi\mathrm{d}r\mathrm{d}\theta+\iint Q_r\delta\varphi r\mathrm{d}r\mathrm{d}\theta+$$

$$\int rQ_r\delta w\Big|_0^R\mathrm{d}\theta-\iint\frac{\partial(rQ_r)}{\partial r}\delta w\mathrm{d}r\mathrm{d}\theta \qquad (30)$$

where V represents the volume occupied by the circular nanoplate. The first-order variation of the kinetic energy T can be determined as

$$\delta T=\delta\int_v\frac{1}{2}\rho\left[\left(\frac{\partial u_r}{\partial t}\right)^2+\left(\frac{\partial u_z}{\partial t}\right)^2\right]\mathrm{d}V=$$

$$\iint\left(I_0\frac{\partial w}{\partial t}\delta\frac{\partial w}{\partial t}+I_2\frac{\partial\varphi}{\partial t}\delta\frac{\partial\varphi}{\partial t}\right)r\mathrm{d}r\mathrm{d}\theta \qquad (31)$$

$$I_0=\int_{-\frac{h}{2}}^{\frac{h}{2}}\rho\mathrm{d}z=\rho h \qquad (32)$$

$$I_2=\int_{-\frac{h}{2}}^{\frac{h}{2}}\rho z^2\mathrm{d}z=\frac{\rho h^3}{12} \qquad (33)$$

where ρ is the bulk density of the circular nanoplate. The variation of the potential energy H caused by the rotation is

$$\delta H=\delta\iint\frac{1}{2}N^R\left(\frac{\partial w}{\partial r}\right)^2 r\mathrm{d}r\mathrm{d}\theta=\iint N^R\frac{\partial w}{\partial r}\delta\frac{\partial w}{\partial r}r\mathrm{d}r\mathrm{d}\theta \qquad (34)$$

where N^R is the radial tension caused by the rotation. For the fixed and simply supported boundary constraints, N^R can be derived as[33]

$$N^R=\frac{3+\nu}{8}\rho h\Omega^2 R^2\left(\frac{1+\nu}{3+\nu}-\frac{r^2}{R^2}\right) \qquad (35)$$

Based on Hamilton's principle, the equation of motion that governs the free out-of-plane vibration of rotating axisymmetric circular nanoplates can be derived as

$$\frac{1}{r}\frac{\partial(rQ_r)}{\partial r}-\frac{1}{r}\frac{\partial}{\partial r}\left(rN^R\frac{\partial w}{\partial r}\right)=I_0\frac{\partial^2 w}{\partial t^2} \qquad (36)$$

$$\frac{1}{r}\frac{\partial(rM_r)}{\partial r}-\frac{M_\theta}{r}-Q_r=I_2\frac{\partial^2\varphi}{\partial t^2} \qquad (37)$$

Substituting Eqs.(22—26) into Eqs.(36,37), the vibration governing equation of the rotating axisymmetric circular nanoplate in the framework of the nonlocal strain gradient theory is

$$(1-l^2\nabla^2)\left[\frac{S_1}{\kappa}\left(\frac{\partial\varphi}{\partial r}+\frac{\varphi}{r}+\frac{\partial^2 w}{\partial r^2}+\frac{1}{r}\frac{\partial w}{\partial r}\right)\right]-$$

$$\left[1-(ea)^2\nabla^2\right]I_0\frac{\partial^2 w}{\partial t^2}-\frac{3+\nu}{8}\rho h\Omega^2 R^2\left[1-\right.$$

$$(ea)^2\nabla^2\left]\left[\left(\frac{1}{r}\frac{1+\nu}{3+\nu}-\frac{3r}{R^2}\right)\frac{\partial w}{\partial r}+\right.$$

$$\left.\left(\frac{1+\nu}{3+\nu}-\frac{r^2}{R^2}\right)\frac{\partial^2 w}{\partial r^2}\right]=0 \qquad (38)$$

$$(1 - l^2\nabla^2)\left[D_1\left(\frac{\partial^2\varphi}{\partial r^2} + \frac{1}{r}\frac{\partial\varphi}{\partial r} - \frac{\varphi}{r^2}\right) - \right.$$

$$\left. \frac{S_1}{\kappa}\left(\varphi + \frac{\partial w}{\partial r}\right)\right] - \left[1 - (ea)^2\nabla^2\right]I_2\frac{\partial^2\varphi}{\partial t^2} = 0 \quad (39)$$

The classical out-of-plane vibration model of a rotating circular plate is recovered in case of $ea = l = 0$. The dimensionless quantities are introduced

$$\bar{w} = \frac{w}{R}, \bar{r} = \frac{r}{R}, b = \frac{h}{R}, \tau = \frac{ea}{R}$$

$$\zeta = \frac{l}{R}, \bar{t} = \frac{t}{R^2}\sqrt{\frac{D_1}{\rho h}}, \lambda = R^2\Omega\sqrt{\frac{\rho h}{D_1}} \quad (40)$$

After that, dimensionless forms of Eqs. (38, 39) can be obtained as

$$(1 - \zeta^2\bar{\nabla}^2)\left[\frac{6(1-\nu)}{\kappa b^2}\left(\frac{\partial\varphi}{\partial\bar{r}} + \frac{\varphi}{\bar{r}} + \frac{\partial^2\bar{w}}{\partial\bar{r}^2} + \right.\right.$$

$$\left.\frac{1}{\bar{r}}\frac{\partial\bar{w}}{\partial\bar{r}}\right)\right] - (1 - \tau^2\bar{\nabla}^2)\frac{\partial^2\bar{w}}{\partial\bar{t}^2} - \frac{3+\nu}{8}\lambda^2\cdot$$

$$(1 - \tau^2\bar{\nabla}^2)\left[\left(\frac{1}{\bar{r}}\frac{1+\nu}{3+\nu} - 3\bar{r}\right)\frac{\partial\bar{w}}{\partial\bar{r}} + \right.$$

$$\left.\left(\frac{1+\nu}{3+\nu} - \bar{r}^2\right)\frac{\partial^2\bar{w}}{\partial\bar{r}^2}\right] = 0 \quad (41)$$

$$(1 - \zeta^2\bar{\nabla}^2)\left[\left(\frac{\partial^2\varphi}{\partial\bar{r}^2} + \frac{1}{\bar{r}}\frac{\partial\varphi}{\partial\bar{r}} - \frac{\varphi}{\bar{r}^2}\right) - \frac{6(1-\nu)}{\kappa b^2}\left(\varphi + \right.\right.$$

$$\left.\left.\frac{\partial\bar{w}}{\partial\bar{r}}\right)\right] - \frac{b^2}{12}(1 - \tau^2\bar{\nabla}^2)\frac{\partial^2\varphi}{\partial\bar{t}^2} = 0 \quad (42)$$

The solutions of Eqs.(41,42) can be set as

$$\bar{w}(\bar{r}, \bar{t}) = \tilde{w}(\bar{r})e^{j\omega\bar{t}}, \quad \varphi(\bar{r}, \bar{t}) = \tilde{\varphi}(\bar{r})e^{j\omega\bar{t}} \quad (43)$$

where $\tilde{w}(\bar{r})$ and $\tilde{\varphi}(\bar{r})$ are the vibration mode functions and ω is the non-dimensional natural frequency of the free out-of-plane vibration.

Substituting Eq.(43) into Eqs.(41, 42), one gets

$$(1 - \zeta^2\bar{\nabla}^2)\left[\frac{6(1-\nu)}{\kappa b^2}\left(\frac{\partial\tilde{\varphi}}{\partial\bar{r}} + \frac{\tilde{\varphi}}{\bar{r}} + \frac{\partial^2\tilde{w}}{\partial\bar{r}^2} + \right.\right.$$

$$\left.\frac{1}{\bar{r}}\frac{\partial\tilde{w}}{\partial\bar{r}}\right)\right] + \omega^2(1 - \tau^2\bar{\nabla}^2)\tilde{w} - \frac{3+\nu}{8}\lambda^2\left(1 - \right.$$

$$\tau^2\bar{\nabla}^2)\left[\left(\frac{1}{\bar{r}}\frac{1+\nu}{3+\nu} - 3\bar{r}\right)\frac{\partial\tilde{w}}{\partial\bar{r}} + \right.$$

$$\left(\frac{1+\nu}{3+\nu} - \bar{r}^2\right)\frac{\partial^2\tilde{w}}{\partial\bar{r}^2}\right] = 0 \quad (44)$$

$$(1 - \zeta^2\bar{\nabla}^2)\left[\left(\frac{\partial^2\tilde{\varphi}}{\partial\bar{r}^2} + \frac{1}{\bar{r}}\frac{\partial\tilde{\varphi}}{\partial\bar{r}} - \frac{\tilde{\varphi}}{\bar{r}^2}\right) - \right.$$

$$\left.\frac{6(1-\nu)}{\kappa b^2}\left(\tilde{\varphi} + \frac{\partial\tilde{w}}{\partial\bar{r}}\right)\right] + \frac{b^2}{12}\omega^2(1 - \tau^2\bar{\nabla}^2)\tilde{\varphi} = 0$$

$$(45)$$

The boundary conditions are

$$\bar{r} = 0: \tilde{\varphi} = 0, \quad \tilde{\varphi} + \frac{\partial\tilde{w}}{\partial\bar{r}} = 0$$

$$\bar{r} = 1: \begin{cases} \text{Fixed} \quad \tilde{w} = 0, \quad \tilde{\varphi} = 0 \\ \text{Simply supported} \quad \frac{\partial\tilde{\varphi}}{\partial\bar{r}} + \nu\frac{\tilde{\varphi}}{\bar{r}} = 0, \quad \tilde{w} = 0 \end{cases}$$

$$(46)$$

Using the differential quadrature method, we can discretize Eqs.(44,45) as

$$\frac{6(1-\nu)}{\kappa b^2}\left[-\zeta^2\sum_{m=1}^{N}C_{jm}^{(3)}\tilde{\varphi}_m - \frac{2\zeta^2}{\bar{r}_j}\sum_{m=1}^{N}C_{jm}^{(2)}\tilde{\varphi}_m + \right.$$

$$\left(1 + \frac{\zeta^2}{\bar{r}_j^{\ 2}}\right)\sum_{m=1}^{N}C_{jm}^{(1)}\tilde{\varphi}_m + \left(\frac{1}{\bar{r}_j} - \frac{\zeta^2}{\bar{r}_j^{\ 3}}\right)\tilde{\varphi}_j\right] +$$

$$\frac{6(1-\nu)}{\kappa b^2}\left[-\zeta^2\sum_{m=1}^{N}C_{jm}^{(4)}\tilde{w}_m - \frac{2\zeta^2}{\bar{r}_j}\sum_{m=1}^{N}C_{jm}^{(3)}\tilde{w}_m + \right.$$

$$\left(1 + \frac{\zeta^2}{\bar{r}_j^{\ 2}}\right)\sum_{m=1}^{N}C_{jm}^{(2)}\tilde{w}_m + \left(\frac{1}{\bar{r}_j} - \frac{\zeta^2}{\bar{r}_j^{\ 3}}\right)\sum_{m=1}^{N}C_{jm}^{(1)}\tilde{w}_m\right] -$$

$$\frac{3+\nu}{8}\lambda^2\left\{\left(\frac{1}{\bar{r}_j}\frac{1+\nu}{3+\nu} - 3\bar{r}_j\right)\sum_{m=1}^{N}C_{jm}^{(1)}\tilde{w}_m + \right.$$

$$\left(\frac{1+\nu}{3+\nu} - \bar{r}_j^{\ 2}\right)\sum_{m=1}^{N}C_{jm}^{(2)}\tilde{w}_m -$$

$$\tau^2\left[\left(\frac{1+\nu}{3+\nu} - \bar{r}_j^{\ 2}\right)\sum_{m=1}^{N}C_{jm}^{(4)}\tilde{w}_m + \right.$$

$$\left(\frac{2}{\bar{r}_j}\frac{1+\nu}{3+\nu} - 8\bar{r}\right)\sum_{m=1}^{N}C_{jm}^{(3)}\tilde{w}_m +$$

$$\left(-\frac{1}{\bar{r}_j^{\ 2}}\frac{1+\nu}{3+\nu} - 13\right)\sum_{m=1}^{N}C_{jm}^{(2)}\tilde{w}_m +$$

$$\left.\left(\frac{1}{\bar{r}_j^{\ 3}}\frac{1+\nu}{3+\nu} - \frac{3}{\bar{r}_j}\right)\sum_{m=1}^{N}C_{jm}^{(1)}\tilde{w}_m\right]\right\} +$$

$$\omega^2\left[\tilde{w}_j - \tau^2\left(\sum_{m=1}^{N}C_{jm}^{(2)}\tilde{w}_m + \frac{1}{\bar{r}_j}\sum_{m=1}^{N}C_{jm}^{(1)}\tilde{w}_m\right)\right] = 0$$

$$(47)$$

$$\frac{6(1-\nu)}{\kappa b^2}\left(\zeta^2\sum_{m=1}^N C_{jm}^{(3)}\tilde{w}_m+\zeta^2\frac{1}{\bar{r}_j}\sum_{m=1}^N C_{jm}^{(2)}\tilde{w}_m-\right.$$

$$\sum_{m=1}^N C_{jm}^{(1)}\tilde{w}_m+\zeta^2\sum_{m=1}^N C_{jm}^{(2)}\tilde{\varphi}_m+$$

$$\left.\zeta^2\frac{1}{\bar{r}_j}\sum_{m=1}^N C_{jm}^{(1)}\tilde{\varphi}_m-\tilde{\varphi}_j\right)+\left[-\zeta^2\sum_{m=1}^N C_{jm}^{(4)}\tilde{\varphi}_m-\right.$$

$$\frac{2\zeta^2}{\bar{r}_j}\sum_{m=1}^N C_{jm}^{(3)}\tilde{\varphi}_m+\left(1+\frac{2\zeta^2}{\bar{r}_j^2}\right)\sum_{m=1}^N C_{jm}^{(2)}\tilde{\varphi}_m+$$

$$\left(\frac{1}{\bar{r}_j}-\frac{4\zeta^2}{\bar{r}_j^3}\right)\sum_{m=1}^N C_{jm}^{(1)}\tilde{\varphi}_m+\left(-\frac{1}{\bar{r}_j^2}+\frac{4\zeta^2}{\bar{r}_j^4}\right)\tilde{\varphi}_j\right]-$$

$$\frac{b^2}{12}\omega^2\left[\tilde{\varphi}_j-\tau^2\left(\sum_{m=1}^N C_{jm}^{(2)}\tilde{\varphi}_m+\frac{1}{\bar{r}_j}\sum_{m=1}^N C_{jm}^{(1)}\tilde{\varphi}_m\right)\right]=0$$

$$(48)$$

where $j=2,3,\cdots,N-1$.

Combining Eqs.(47, 48) and the boundary conditions, the characteristic equation in matrix form can be written as

$$\begin{bmatrix} K_{d1} & K_{d2} \\ K_{b1} & K_{b2} \end{bmatrix}\begin{Bmatrix} q_1 \\ q_2 \end{Bmatrix}-\omega^2\begin{bmatrix} M_{d1} & M_{d2} \\ M_{b1} & M_{b2} \end{bmatrix}\begin{Bmatrix} q_1 \\ q_2 \end{Bmatrix}=\begin{Bmatrix} 0 \\ 0 \end{Bmatrix} \quad (49)$$

where K, M are the stiffness matrix and the mass matrix, respectively. Subscript d represents the governing equations; subscript b the boundary conditions; and q the nodal displacement including the lateral displacement q_1 and the rotational angle q_2. Therefore, K, M are the coefficient matrices with respect to the lateral displacement and the rotational angle. The elements of the matrix consist of different equations that are associated with parameters ζ, b and so on. The expression of each element in the matrix is rather lengthy and is not specifically listed here.

3   Results and Discussion

In order to verify the effectiveness of the proposed calculation method, a simplified case of the present model, that is, the free vibration of a non-rotating circular macro-plate, is discussed herein. Let $\tau=\zeta=\lambda=0$. We can determine the first three natural frequencies of the circular nanoplate with different ratios of thickness to radius under the fixed and simply supported boundary conditions according to Eqs.(47, 48), which are compared with the results available in Ref.[34], as shown in Tables 1, 2.

From Tables 1, 2, the presented results are very close to those in Ref.[34]. Accordingly, the solution method and the numerical results are validated. Besides, with an increase of the thickness to radius ratio (e.g. from $b=0.05$ to $b=0.2$), there is a decrease in the natural frequency. Note that reducing of the natural frequency means the nanostructural stiffness weakening. However, increasing the thickness to radius ratio corresponds to increasing the thickness or decreasing the radius. Increasing the thickness means increasing the nanostructural stiffness, while decreasing the radius means decreasing the nanostructural stiffness. As from the two aspects, one can infer that the stiffness weakening effect caused by decreasing the radius is greater than the stiffness enhancement effect caused by increasing the thickness. This is because only in this way the stiffness of the circular nanoplate will eventually

Table 1   Comparison of the first three natural frequencies of the circular plate under the fixed boundary condition

Mode	$b=0.05$		$b=0.1$		$b=0.15$		$b=0.2$	
	The presented	Ref.[34]	The presented	Ref.[34]	The presented	Ref.[34]	The presented	Ref.[34]
1	10.143	10.145	9.940 6	9.940 8	9.628 3	9.628 6	9.240 0	9.240 0
2	38.852	38.855	36.473	36.479	33.392	33.393	30.208	30.211
3	84.992	84.995	75.661	75.664	65.547	65.551	56.677	56.682

Table 2   Comparison of the first three natural frequencies of the circular plate under the simply supported boundary condition

Mode	$b=0.05$		$b=0.1$		$b=0.15$		$b=0.2$	
	The presented	Ref.[34]	The presented	Ref.[34]	The presented	Ref.[34]	The presented	Ref.[34]
1	4.924 3	4.924 7	4.893 2	4.893 8	4.843 6	4.844 0	4.777 0	4.777 3
2	29.320	29.323	28.238	28.240	26.711	26.715	24.991	24.994
3	71.751	71.756	65.936	65.942	59.058	59.062	52.509	52.514

reduce. Moreover, the natural frequencies under fixed support conditions are higher than those under simply supported ones.

Considering a circular nanoplate made of ceramics (Si_3N_4) with the thickness $h=2.5$ nm, radius $R=50$ nm, density $\rho_c=2\ 370$ kg/m^3, elastic modulus $E_c=348.43$ GPa, and Poisson's ratio $\nu=0.3$. Node $N=18$ is selected in the numerical calculations, and we examine the vibration characteristics of the rotating axisymmetric circular nanoplate with the fixed and simply supported outer boundary constraints.

The effect of the thickness to radius ratio b on the first three dimensionless natural frequencies of the circular nanoplate is shown in Fig.2, where $ea=0.5$ nm, $l=1$ nm, $\tau=0.01$ and $\zeta=0.02$. The natural frequency decreases with the increase of the thickness to radius ratio, and the higher-order vibration is affected more obviously by the change of the thickness to radius ratio.

The natural frequencies versus the angular velocity λ, the nonlocal characteristic scale parameter ea, and the material characteristic scale parameter l

are shown in Figs.3—6. The nonlocal and material characteristic scale parameters represent the nonlocal and strain gradient effects, respectively, and are selected as zero in Fig.3, and the out-of-plane vibration of the rotating axisymmetric circular plate or the classical model can be recovered. From Fig.3(a), it can be seen that natural frequencies with the peripheral fixed boundaries decrease with the increasing angular velocity. When the angular velocity increases to $\lambda_1=15.689$, the first natural frequency becomes zero which indicates that the vibration of the rotating circular plate appears divergent instability. So $\lambda_1=15.689$ is called the first-order critical angular velocity. Similarly, $\lambda_2=30.307$ is the second-order critical angular velocity. From Fig.3(b), one can see that the first natural frequency of the peripheral simply supported case does not decrease monotonously with the increase of the angular velocity, which is different from the peripheral fixed constraint, and the boundary effect in the out-of-plane vibration of the rotating axisymmetric circular plate is thus reflected. The instability characteristics are
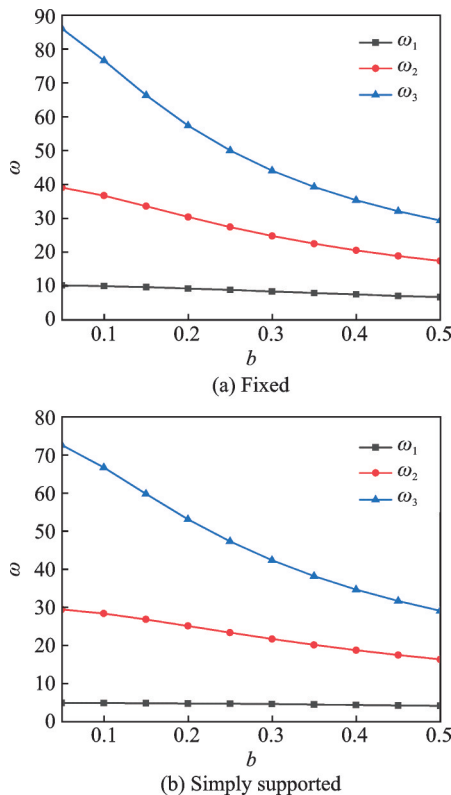

Fig.2   Influence of the thickness to radius ratio on natural frequencies ($\tau=0.01$, $\zeta=0.02$, $\lambda=0$)
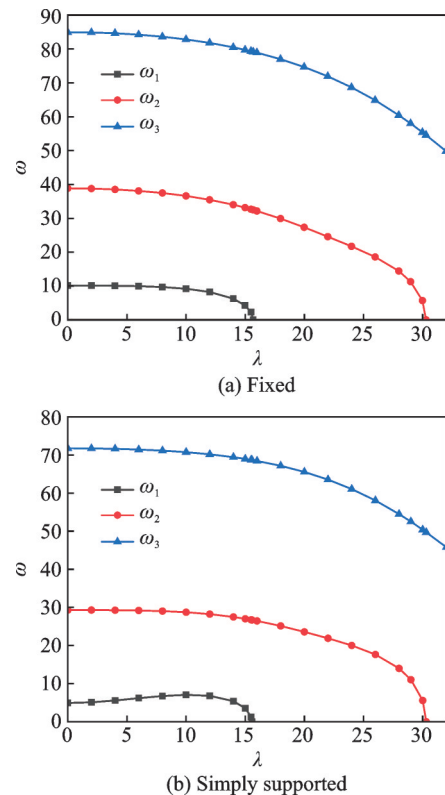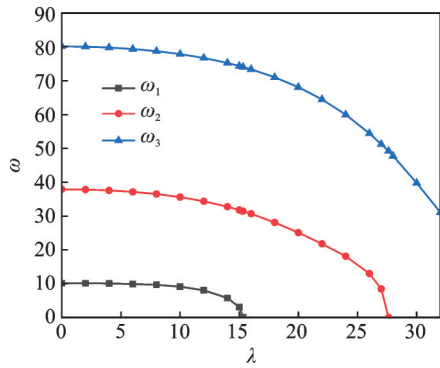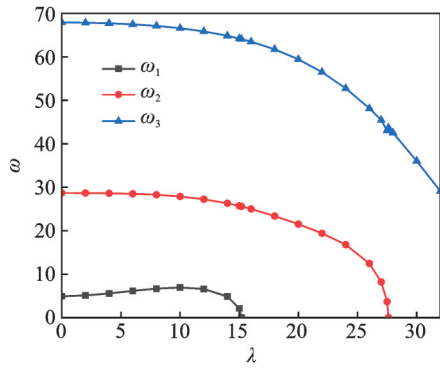

Fig.3   Influence of the dimensionless angular velocity on natural frequencies ($\tau=\zeta=0$)
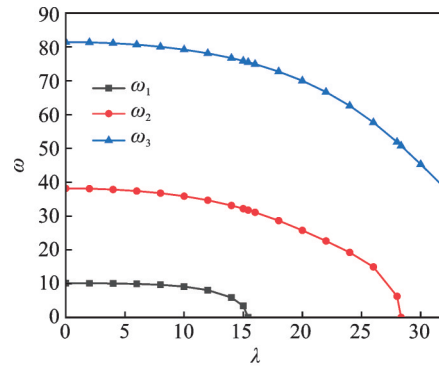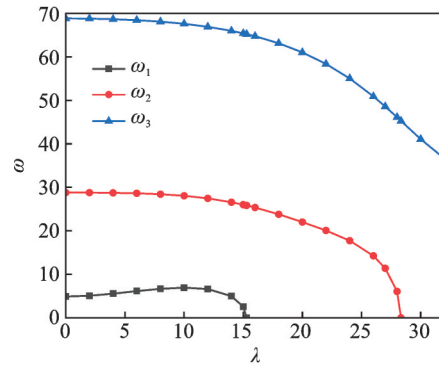
(a) Fixed

(b) Simply supported

Fig.4 Influence of the dimensionless angular velocity on natural frequencies ($\tau=0.04$, $\zeta=0$)
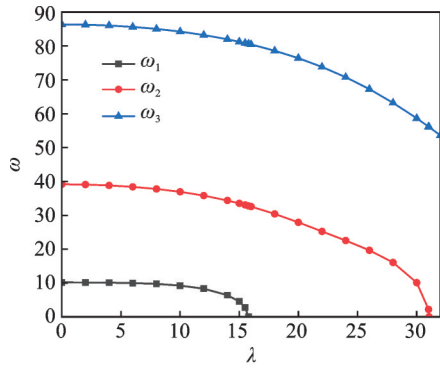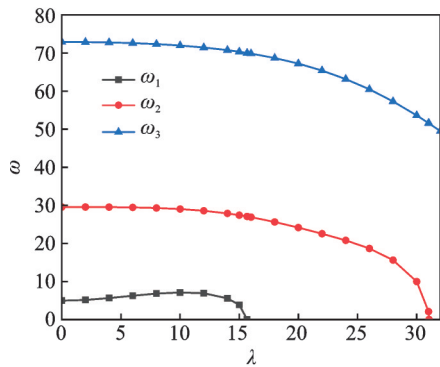

(a) Fixed

(b) Simply supported

Fig.6 Influence of the dimensionless angular velocity on natural frequencies ($\tau=0.04$, $\zeta=0.02$)

(a) Fixed

(b) Simply supported

Fig.5 Influence of the dimensionless angular velocity on natural frequencies ($\tau=0$, $\zeta=0.02$)

the same as those of the peripheral fixed rotating circular nanoplate.

Comparing the results from Figs.3—6, we find that the natural frequency decreases with the increasing nonlocal characteristic scale parameter. The decrease of natural frequencies means a stiffness weakening of structures. Hence it is demonstrated that the nonlocal characteristic scale has a softening effect on the nanostructure. In Fig.4(a), the first-order critical angular velocity decreases from 15.689 to 15.324, and the second-order decreases from 30.307 to 27.626 with the increase of the nonlocal characteristic scale parameter. This means the nonlocal characteristic scale makes the critical angular velocity decrease. In fact, such an observation is also one of the manifestations of the nonlocal softening effect. Fig.5(a) shows that the natural frequency increases with the increase of the material characteristic scale parameter, so the strain gradient has a hardening effect on the nanostructure. With the increase of the material characteristic scale parameter, the first-order and the second-order critical angular velocities increase from 15.689 to 15.783 and from 30.307 to 31.046, respectively. This indicates that the existence of the material characteristic scale in-

creases the critical angular velocity and the strain gradient hardening effect is revealed again.

To reveal the relationship between the nonlocal scale and strain gradient effects in the out-of-plane vibration of the rotating axisymmetric circular nanoplate, we display the effect of the ratio ea/l on the first three natural frequencies, as shown in Fig.7. As observed, the natural frequency decreases with the increase of ea/l. As mentioned before, the theoretical model will degenerate to the classical counterpart when ea and l are both equal to zero. In fact, this condition can be relaxed. As long as ea is equal to l, even if both are not zero, the natural frequencies keep unchanged with respect to the ratio ea/l. Consequently, the results are always equal to those

of the classical counterpart, and both the softening and hardening phenomena disappear, which shows that the softening/hardening effects derived from the two internal characteristic scale parameters on the nanostructures can cancel each other. This implies that the nonlocal scale effect and strain gradient effect have the opposite mechanisms in nanostructures, but the degree of effects is equivalent. When ea/l is less than 1, that is, ea is less than l, the natural frequencies based on the nonlocal strain gradient theory is greater than those based on the classical vibration theory, and the larger the material characteristic scale parameter, the greater the degree of deviation from the classical results. In this instance, the characteristic scale parameters strength-
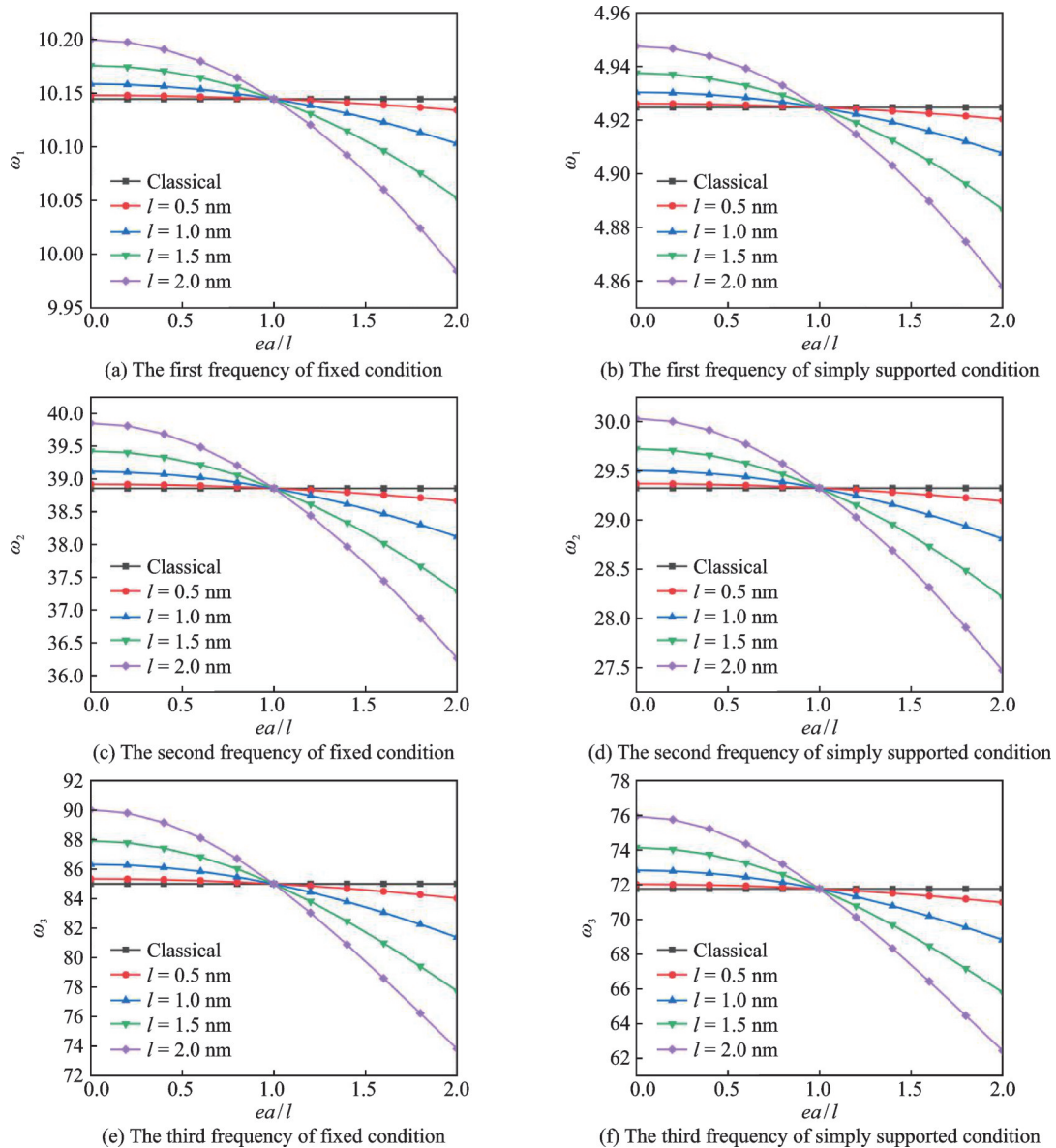

(a) The first frequency of fixed condition

(b) The first frequency of simply supported condition

(c) The second frequency of fixed condition

(d) The second frequency of simply supported condition

(e) The third frequency of fixed condition

(f) The third frequency of simply supported condition

Fig.7　Relationship between ea/l and the dimensionless natural frequency ($\lambda=0$)

en the stiffness of the rotating circular nanoplate. However, when ea/l is greater than 1, that is, ea is greater than l, the natural frequency based on the nonlocal strain gradient theory is less than their classical counterparts, and the larger the material characteristic scale parameter is, the more obvious this phenomenon is. So the internal characteristic scale parameters weaken the nanoplate stiffness. Therefore, there is a coupling relationship between the nonlocal and material characteristic scale parameters. The magnitude relationship between the two internal characteristic scale parameters will determine the specific manifestation of the internal scale effects in the nonlocal strain gradient theory, that is, the nonlocal softening or strain gradient hardening phenomenon in the rotating circular nanoplate. When the nonlocal characteristic scale parameter is larger than the material characteristic scale parameter, the nonlocal softening effect plays a dominated role in the nonlocal strain gradient theory. Otherwise, the strain gradient hardening effect dominates the internal characteristic scale effects

4   Conclusions

The out-of-plane vibration analyses of the rotating axisymmetric circular nanoplate is carried out based on the nonlocal strain gradient theory and the Mindlin plate model. The governing differential equation of motion that includes the nonlocal and material characteristic scale effects is derived, and the natural frequency is calculated by the differential quadrature method. The natural frequency decreases with the increase of the thickness to radius ratio, and the higher-order frequencies are influenced more significantly. The natural frequency decreases with the increase of the angular velocity. When the angular velocity increases to a critical value, the natural frequency becomes zero. The critical angular velocity is greatly affected by the internal characteristic scale parameters. The existence of the nonlocal characteristic scale parameter reduces the critical angular velocity, but the existence of the material characteristic scale parameter causes it to increase. The stiff-

ness of the circular nanoplate decreases with the increase of the nonlocal characteristic scale parameter, but increases with the increase of the material characteristic scale parameter. The two internal scale parameters are coupled in the nonlocal strain gradient theory. The parameter with a larger value is dominant in the internal characteristic scale effects.

References

[1] YAN J W, LIEW K M, HE L H. Ultra-sensitive analysis of a cantilevered single-walled carbon nano-cone-based mass detector[J]. Nanotechnology, 2013, 24(12): 125703.

[2] JIANG J N, WANG L F, ZHANG Y Q. Vibration of single-walled carbon nanotubes with elastic boundary conditions[J]. International Journal of Mechanical Sciences, 2017, 122: 156-166.

[3] MASARA B, POLL J A, MAAZA M. The "Nanotechnology Innovation Diamond": A model for successful nanoscience research and development[J]. Journal of Nanoparticle Research, 2021, 23(3): 1-15.

[4] SUN J, MURUGANATHAN M, KANETAKE N, et al. Locally-actuated graphene-based nano-electro-mechanical switch[J]. Micromachines, 2016, 7 (7): 124.

[5] MACHADO L D, BIZAO R A, PUGNO N M, et al. Controlling movement at nanoscale: Curvature driven mechanotaxis[J]. Small, 2021, 17(35): e2100909.

[6] SHEN J P, WANG P Y, LI C, et al. New observations on transverse dynamics of microtubules based on nonlocal strain gradient theory[J]. Composite Structures, 2019, 225: 111036.

[7] ZAKOMIRNYI V I, RASSKAZOV I L, SØRENSEN L K, et al. Plasmonic nano-shells: Atomistic discrete interaction versus classic electrodynamics models[J]. Physical Chemistry Chemical Physics, 2020, 22(24): 13467-13473.

[8] XIA W, WANG L, YIN L. Nonlinear non-classical microscale beams: Static bending, postbuckling and free vibration[J]. International Journal of Engineering Science, 2010, 48(12): 2044-2053.

[9] DEHROUYEH-SEMNANI A M. A discussion on different non-classical constitutive models of micro-beam[J]. International Journal of Engineering Science, 2014, 85: 66-73.

[10] AKGÖZ B, CIVALEK O. A size-dependent shear de-

formation beam model based on the strain gradient elasticity theory[J]. International Journal of Engineering Science, 2013, 70: 1-14.

[11] AKGÖZ B, CIVALEK O. Thermo-mechanical buckling behavior of functionally graded microbeams embedded in elastic medium[J]. International Journal of Engineering Science, 2014, 85: 90-104.

[12] NUMANOĞLU H M, AKGÖZ B, CIVALEK O. On dynamic analysis of nanorods[J]. International Journal of Engineering Science, 2018, 130: 33-50.

[13] EBRAHIMI F, BARATI M R, CIVALEK O. Application of Chebyshev-Ritz method for static stability and vibration analysis of nonlocal microstructure-dependent nanostructures[J]. Engineering with Computers, 2020, 36(3): 953-964.

[14] LIM C W, YANG Y. New predictions of size-dependent nanoscale based on non local elasticity for wave propagation in carbon nanotubes[J]. Journal of Computational and Theoretical Nanoscience, 2010, 7(6): 988-995.

[15] LI C, SUI S H, CHEN L, et al. Nonlocal elasticity approach for free longitudinal vibration of circular truncated nanocones and method of determining the range of nonlocal small scale[J]. Smart Structures and Systems, 2018, 21(3): 279-286.

[16] LIM C W, ZHANG G, REDDY J N. A higher-order nonlocal elasticity and strain gradient theory and its applications in wave propagation[J]. Journal of the Mechanics and Physics of Solids, 2015, 78: 298-313.

[17] LI L, HU Y J. Nonlinear bending and free vibration analyses of nonlocal strain gradient beams made of functionally graded material[J]. International Journal of Engineering Science, 2016, 107: 77-97.

[18] LI C, LAI S K, YANG X. On the nano-structural dependence of nonlocal dynamics and its relationship to the upper limit of nonlocal scale parameter[J]. Applied Mathematical Modelling, 2019, 69: 127-141.

[19] LU L, GUO X M, ZHAO J Z. Size-dependent vibration analysis of nanobeams based on the nonlocal strain gradient theory[J]. International Journal of Engineering Science, 2017, 116: 12-24.

[20] SHAFIEI N, SHE G L. On vibration of functionally graded nano-tubes in the thermal environment[J]. International Journal of Engineering Science, 2018, 133: 84-98.

[21] CHEN W, WANG L, DAI H L. Nonlinear free vibration of nanobeams based on nonlocal strain gradient theory with the consideration of thickness-dependent size effect[J]. Journal of Mechanics of Materials and Structures, 2019, 14(1): 119-137.

[22] THAI C H, FERREIRA A J M, PHUNG-VAN P. A nonlocal strain gradient isogeometric model for free vibration and bending analyses of functionally graded plates[J]. Composite Structures, 2020, 251: 112634.

[23] LI C, QING H, GAO C F. Theoretical analysis for static bending of Euler-Bernoulli using different nonlocal gradient models[J]. Mechanics of Advanced Materials and Structures, 2021, 28(19): 1965-1977.

[24] FAGHIDIAN S A, ZUR K K, REDDY J N. A mixed variational framework for higher-order unified gradient elasticity[J]. International Journal of Engineering Science, 2022, 170: 103603.

[25] LIM C W, LI C, YU Y J. Dynamic behaviour of axially moving nanobeams based on nonlocal elasticity approach[J]. Acta Mechanica Sinica, 2010, 26(5): 755-765.

[26] LI C. Size-dependent thermal behaviors of axially traveling nanobeams based on a strain gradient theory[J]. Structural Engineering and Mechanics, 2013, 48(3): 415-434.

[27] MOKHTARI A, MIRDAMADI H R, GHAYOUR M, et al. Time/wave domain analysis for axially moving pre-stressed nanobeam by wavelet-based spectral element method[J]. International Journal of Mechanical Sciences, 2016, 105: 58-69.

[28] WANG J, SHEN H M, ZHANG B, et al. Complex modal analysis of transverse free vibrations for axially moving nanobeams based on the nonlocal strain gradient theory[J]. Physica E: Low-Dimensional Systems and Nanostructures, 2018, 101: 85-93.

[29] LI C, WANG P Y, LUO Q Y, et al. Free vibration of axially moving functionally graded nanoplates based on the nonlocal strain gradient theory[J]. International Journal of Acoustics and Vibration, 2020, 25(4): 587-596.

[30] ZHAO X, WANG C F, ZHU W D, et al. Coupled thermoelastic nonlocal forced vibration of an axially moving micro/nano-beam[J]. International Journal of Mechanical Sciences, 2021, 206: 106600.

[31] SHI J, WANG Z Z, CHEN Z. Concurrence of oscillatory and rotation of the rotors in a thermal nanotube motor[J]. Computational Materials Science, 2016, 120: 94-98.

[32] SHERBOURNE A N, PANDEY M D. Differential quadrature method in the buckling analysis of beams and composite plates[J]. Computers & Structures, 1991, 40(4): 903-913.

[33] YANG Y Q, WANG Z M, WANG Y Q. Thermo-

elastic coupling vibration and stability analysis of rotating circular plate in friction clutch[J]. Journal of Low Frequency Noise, Vibration and Active Control, 2019, 38(2): 558-573.

[34] LIEW K M, HAN J B, XIAO Z M. Vibration analysis of circular mindlin plates using the differential quadrature method[J]. Journal of Sound and Vibration, 1997, 205(5): 617-630.

[35] WANG C M, REDDY J N, LEE K H. Shear deformable beams and plates: Relationships with classical solutions[M]. Oxford, UK: Elsevier Science Ltd, 2000.

Authors Ms. **WANG Xinyue** received her bachelor degree in Vehicle Engineering from Soochow University. She is currently a postgraduate of the School of Rail Transportation, Soochow University, Suzhou, China. Her research is focused on metamaterials, smart structures and their applications in vehicle dynamics and control.

Prof. **LI Cheng** is a professor of the School of Rail Transportation, Soochow University, Suzhou, China. He received his Ph.D degree in Engineering Mechanics from Department of Architecture and Civil Engineering, City University of Hong Kong. His research interests include structural mechanics, nonlinear vibration of engineering structures, and vehicle dynamics and control.

Author contributions Ms. **WANG Xinyue** designed the study, analyzed the results, investigated literature and wrote the manuscript. Mr. **LUO Qiuyang** conducted calculation, drew the image, and collated the results. Prof. **LI Cheng** was responsible for supervision and provided methods and resources. Prof. **XIE Zhongyou** contributed to the discussion and background of the study. All authors commented on the manuscript draft and approved the submission.

Competing interests The authors declare no competing interests.

（Production Editor：ZHANG Bei）

旋转圆形纳米板的面外振动

王馨悦[1]，罗秋阳[1]，李　成[1]，谢中友[2]

（1.苏州大学轨道交通学院,苏州 215131, 中国；2.铜陵大学建筑工程学院,铜陵 244061, 中国）

摘要：通过结合非局部尺度和应变梯度效应的 Mindlin 板理论对轴对称旋转纳米圆板进行建模。考虑纳米圆板的剪切变形，应用非局部应变梯度理论推导出描述纳米板面外自由振动行为的控制微分运动方程。应用微分求积法对控制方程进行数值求解，从而得到旋转纳米板面外振动的固有频率。在数值算例中考虑了实际工程中常见的两种边界条件，即固定约束和简支约束。分析了固有频率随厚径比、角速度、非局部特征尺度和材料特征尺度的变化。特别地，旋转纳米圆板是否稳定的临界角速度是数值获得的。本研究对当前纳米技术和纳米器件中旋转圆形纳米结构的动态设计和控制具有参考意义。

关键词：纳米圆板；非局部应变梯度；微分求积法；材料特征尺度；角速度